J Mater Sci (2009) 44:5420–5427
DOI 10.1007/s10853-009-3686-2

FERROELECTRICS

Relaxor behavior of $(1 - x)BaTiO_3$–$x(Bi_{3/4}Na_{1/4})(Mg_{1/4}Ti_{3/4})O_3$ $(0.2 \leq x \leq 0.9)$ ferroelectric ceramic

Liying Wu · Xiaoli Wang · Jimmy H. Wang · Ruyan Guo · Amar S. Bhalla

Received: 21 May 2009 / Accepted: 13 June 2009 / Published online: 30 June 2009

Abstract The $(1 - x)BaTiO_3$–$x(Bi_{3/4}Na_{1/4})(Mg_{1/4}Ti_{3/4})O_3$ $(0.2 \leq x \leq 0.9)$ ceramics were prepared by conventional solid-state reaction route. Their dielectric properties were found to follow a modified Curie–Weiss law and an empirical Lorenz-type relation in respective temperature regions. Their dielectric relaxation times fit well with the Vogel–Fulcher relation for $x = 0.2$, 0.3, and 0.4. For $x = 0.5$, 0.6, 0.7, and 0.8, however, the fitting curves of Vogel–Fulcher relation showed certain deviation from the experimental data. Based on the theoretical treatment of Landau–Ginsburg–Devonshire theory, an approximate treatment of the *E*-field dependence of the permittivity was adopted and found to describe well the field dependence of the permittivity for $x = 0.3$ at temperatures equal to and below T_m (temperature of maximum dielectric permittivity). A combined Langevin-type expression used in the present work appears to give a good account for the field dependence of the permittivity, assuming polar regions are of a statistical cluster size. For polar clusters of linear dimension $L \sim 4$–8 nm for instance, the fitted values of polarization are in the range of $P \sim 6.2$–9.8 μC/cm^2.

Introduction

Cationic substitutions on the A- or B-site in the barium titanate (BT), an environmental friendly lead-free material, have received renewed attention for the purpose of tailoring the ferroelectric relaxor properties. A wide range of frequency-agile properties such as high dielectric permittivities (for tunable multilayer ceramic capacitors) and high electromechanical strains (for wide bandwidth actuators) can be then obtained. In recent years, despite remarkable progresses on studying fundamental physics of relaxor have been achieved [1, 2], the mechanism leading to the relaxor behavior is still an issue open for interpretation. In a classical relaxor, e.g., $Pb(Mg_{1/3}Nb_{2/3})O_3$ (PMN) [3], there is a local imbalance of ionic charge due to Mg^{2+} and Nb^{5+} occupancies at the B-site giving rise to intense random fields. Isovalent substitution, on the other hand, does not lead to such a local charge imbalance. It is well demonstrated in the $BaZr_xTi_{1-x}O_3$ (BZT) system [4–6] that the relaxor behavior evolves gradually with the increases of the isovalent substitution of Ti^{4+} for the Zr^{4+} ions in the BZT. In solid solution $Ba_{1-x}Sr_xTiO_3$ (BST) where Sr^{2+} substitutes for Ba^{2+} in $BaTiO_3$, reports suggested that the permittivity related to the rhombohedral transition of BT shows relaxor features for $x \geq 0.12$[7–9]. Complex heterovalence ion substitutions on both A- and B-sites of the perovskite oxide $(Bi_{3/4}\ Na_{1/4})(Mg_{1/4}Ti_{3/4})O_3$ (BNMT) also show a ferroelectric relaxor-type behavior (frequency dependent broad dielectric peaks) around its ferroelectric to paraelectric phase transition temperature [10]. The $(1 - x)$ BT–*x*BNMT system ($x = 0$–0.3) exhibits a pinched phase transition at $x = 0.2$, i.e., all the three transitions corresponding to pure BT are merged or pinched into one broad peak of relaxor-type [11].

In the present investigation on $(1 - x)$BT–*x*BNMT ($x = 0.2$–0.9) ceramics, gradual evolution of the relaxor behavior was observed with increasing substitution of BNMT in BT. The electric field dependent permittivity of a selected composition ($x = 0.3$) has been studied. One broad relaxor-

L. Wu (✉) · X. Wang
Department of Material Physics, Xi'an Jiaotong University, Xi'an 710049, China
e-mail: wuliying66@gmail.com

J. H. Wang · R. Guo · A. S. Bhalla
Department of Electrical and Computer Engineering, University of Texas at San Antonio, San Antonio, TX 78249, USA

type frequency-dependent dielectric peak was observed for each of all the compositions studied in $0.2 \leq x \leq 0.9$; however, more than one loss peaks were observed for these compositions. The dielectric relaxations in compositions $0.2 \leq x \leq 0.9$ were found to follow Vogel–Fulcher relation (VF) [12–14]. Based on the dielectric studies of $(1 - x)$BT–xBNMT ceramics, the observed relaxor behavior is hypothesized by the formation of polar BNMT in the polar 0.8BT–0.2BNMT (relaxor-based) matrix. It is suggested that more than one type of polar nanoregions (PNRs) give contributions to the system until the concentration (percolation) limits are reached. If the concentrations of all PNRs are high enough to establish long-range interactions, the composite shows a combined relaxation behavior. The theoretical treatment of Landau–Ginsburg–Devonshire (LGD) theory [15–18] and its approximate treatment of the E-field dependence of the permittivity are discussed in this article. Langevin theory [19] is also introduced in combination with LGD to describe the relaxor behavior observed.

Experimental procedures

The samples of $(1 - x)$BT–xBNMT ceramics ($x = 0.2$–0.9) were prepared by a solid-state reaction technique. X-ray diffraction analysis was carried out using Shimadzu XRD-6000 (Cu-Kα radiation, $2\theta \sim 20$–$80°$) to identify the phase purity of the samples. Gold electrodes were sputtered on the ceramic samples for dielectric measurements. The dielectric constant and tangent loss of each sample were measured in two temperature segments, i.e., a cryogenic system for low temperature range (20–300 K, 2 K/min) and a temperature-controlled chamber for high temperature range (300–600 K, 2 K/min). Dielectric data were measured using HP 4284A LCR meter from 100 Hz to 1 MHz and the data were presented in a combined temperature scale.

For electric field dependent dielectric properties, a DC voltage was applied to the samples and a blocking circuit was adopted to separate the high DC voltage and the LCR meter. At each temperature, the sample was allowed to reach thermal equilibrium (holding for 15 min) before the field dependence of the dielectric constant and loss data were acquired.

Results and discussions

XRD pattern

Figure 1 shows X-ray diffraction (XRD) patterns of the $(1 - x)$BT–x BNMT ceramics ($0.2 \leq x \leq 1$) at room temperature. All the results were verified to be single-phase perovskite structures and can be fitted as pseudo-cubic symmetries within experimental resolution.

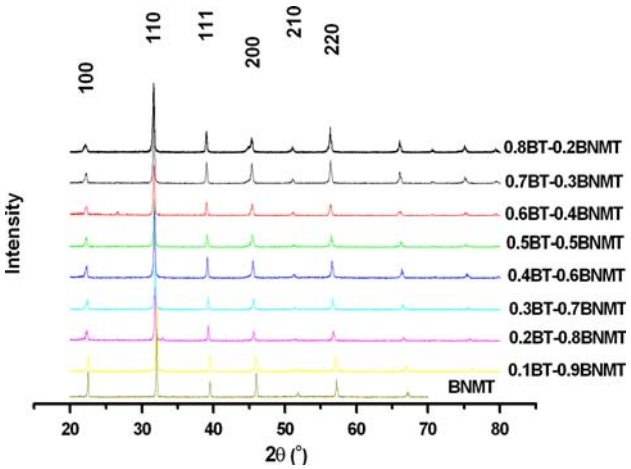

Fig. 1 X-ray diffraction (XRD) patterns of the $(1 - x)$BT–xBNMT ceramics ($0.2 \leq x \leq 1$) at room temperature. All the results were verified to be single-phase perovskite pseudo-cubic structures

Dielectric behavior of $(1 - x)$BT–xBNMT ceramics system ($x = 0.2$–0.9): frequency dependence

The frequency dependence (100 Hz–1 MHz) of permittivity (ε') and loss of $(1 - x)$BT–xBNMT ceramics, with $x = 0.9$, 0.8, 0.6, 0.4, 0.3, and 0.2, are shown in Fig. 2a. One frequency dispersion peak was observed around the T_m (where the dielectric maxima occur) of ε' for all these compositions. Like all ferroelectric relaxors, it is observed that ε' decreases with increasing frequency at a given temperature. In addition, T_m shifts to higher temperatures with increasing frequency for $x = 0.2$–0.9. The frequency dispersions for $x = 0.9$ and $x = 0.8$ at T_m are less pronounced than that of the other compositions. It is also evident that from Fig. 2a, dielectric losses show more than one peaks for $0.9 \leq x \leq 0.4$ (marked as A and B in Fig. 2a). For $x = 0.2$, the dielectric loss curve shows one peak and the peak temperature increases with increasing frequency, which is typical for ferroelectric relaxors. For $x = 0.6$–0.8, the dielectric loss curves show more than one peaks including an additional ripple right below T_m' (where the dielectric loss maxima occur). It is observed that below 150 K, there is almost no frequency dispersion in loss for $x = 0.6$–0.8. Figure 2b shows T_m as a function of composition ($x = 0.2$–0.9) at 10, 100, and 1,000 kHz, respectively. It is observed that T_m for $x = 0.2$–0.9 increases with increasing x for all three frequencies. Moreover, the frequency dispersion of the T_m versus x seems to increase with x initially and tapered off before diminishes at $x \sim 0.9$. Further investigations are in progress to understand the relation of T_m versus composition at different frequencies.

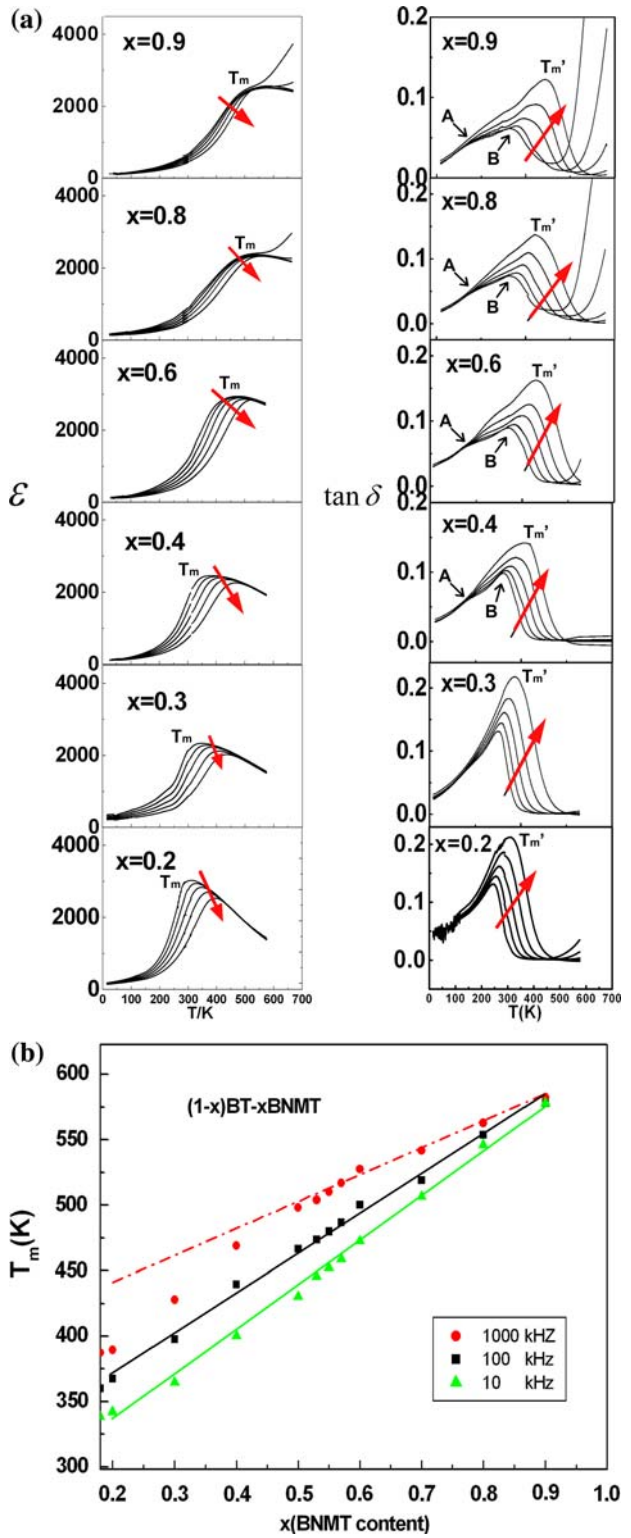

Fig. 2 **a** Dielectric constants and losses as functions of temperature and frequencies for $(1 - x)$BT–xBNMT compositions. Dielectric maxima are denoted as T_m and loss maxima are denoted as T_m'. Two local peaks from loss charts are denoted as A and B. The *arrows* point to the direction of increasing frequencies. **b** T_m as a function of BNMT content in $(1 - x)$BT–xBNMT ceramics system at 10 kHz, 100 kHz, and 1 MHz, respectively

Characteristics of dielectric peaks in $(1 - x)$BT–xBNMT ceramics system ($x = 0.2$–0.9)

To describe the "diffuseness of the phase transition" of relaxor ferroelectrics, a modified Curie–Weiss law [20] was adapted as:

$$\frac{1}{\varepsilon} - \frac{1}{\varepsilon_m} = \frac{(T - T_m)^\gamma}{C_1} \tag{1}$$

where C_1 is the modified Curie–Weiss constant and $1 \leq \gamma \leq 2$. The value γ evolves from $\gamma = 1$ for Curie–Weiss behavior to $\gamma = 2$ for ideal relaxor ferroelectric behavior. Although there is no macroscopic phase change, this empirical relation permits one to find a set of best fitted parameters to describe most ferroelectric relaxors. The fitted values, γ, of the experimental data $(1 - x)$BT–xBNMT ($x = 0.2$–0.9) at 10 kHz, are listed in Table 1. The fitted curves are shown in Fig. 3, for compositions $x = 0.2$–0.9, respectively.

As seen recently from a number of reported relaxors [21, 22], the slope of ε' at $T > T_m$ can be scaled with the empirical Lorenz-type relation:

$$\frac{\varepsilon_A}{\varepsilon} = \frac{(T - T_A)^2}{2\delta^2} \tag{2}$$

where T_A ($<T_m$) and ε_A ($>\varepsilon_m$) are the fitting parameters defining the temperature and magnitude of the Lorenz peak. δ represents the degree of diffuseness of the peak. This equation gives a more agreeable description of the experimental data than the previously used relation $\frac{\varepsilon_m}{\varepsilon} - 1 = \frac{(T-T_m)^\gamma}{2\delta^2}$ [23]. It describes the static conventional relaxor susceptibility, which provides the dominant contribution to the permittivity peak at temperatures above the temperature of the dielectric maximum. In the close vicinity of the peak temperature and below, the magnitude of permittivity drastically decreased due to the on-set of long range order in polarization that curbed contribution from relaxor behavior. All the samples show good agreements to this formula above T_m. A curve fitted by Lorenz-type relation for 0.8BT–0.2BNMT ceramic is shown in Fig. 4 as an example. An excellent fit is obtained for 386 K and above (a little higher than $T_m = 376.6$ K). It is suggested that the deviation of experimental data from the Lorenz relation near T_m is mainly due to the relaxor

Table 1 Fitting values of γ using T_m and ε_m at 10 kHz for various compositions in $(1 - x)$BT–xBNMT ($x \sim 0.2$–0.9) ceramics system

x	0.9	0.8	0.7	0.6	0.5	0.4	0.3	0.2
γ	1.86	1.87	1.90	1.85	1.78	1.85	1.75	1.72
T_m (K)	572.9	546	506.6	472.4	430.2	400	364.5	342.1
ε_m	2517	2343	2725	3155	1751	2386	2410	2832

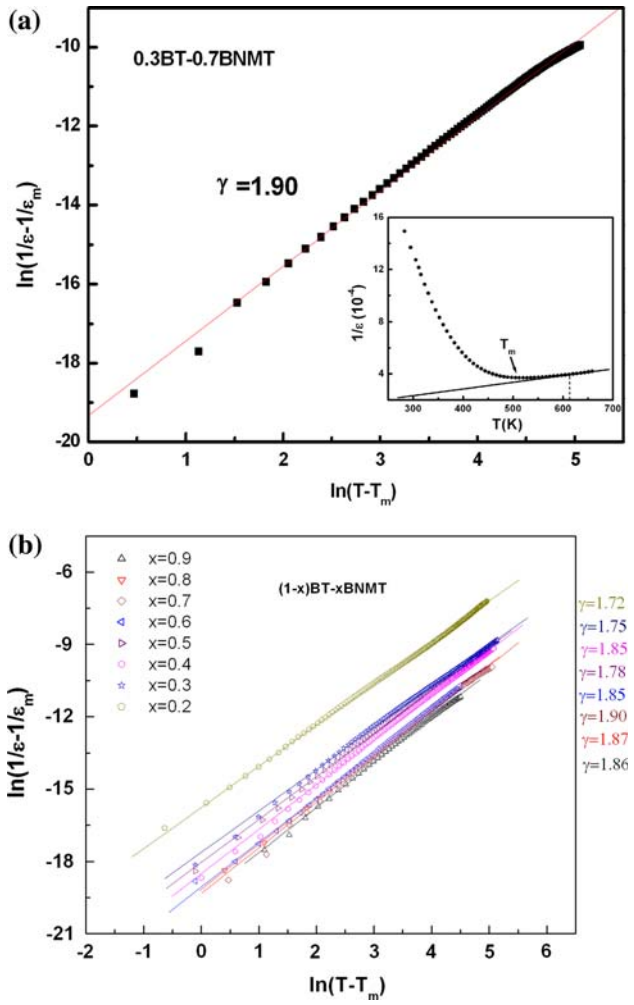

Fig. 3 Plots of $\ln(1/\varepsilon - 1/\varepsilon_m)$ versus $\ln(T - T_m)$ for **a** 0.3BT–0.7BNMT and **b** $(1 - x)$BT–xBNMT ceramics ($x = 0.2$–0.9). *Symbols* denote experimental data and *solid lines* denote fitted trends using Eq. 1. The inset of (**a**) shows the plot of $1/\varepsilon$ versus T for 0.3BT–0.7BNMT. The *solid line*, fitted according to the Curie–Weiss law ($1/\varepsilon = (T - \theta)/C$, where C is the Curie constant, and θ is the Curie–Weiss temperature) is valid at $T > T_m$

dispersion, which becomes significant below 386 K. T_A (337.4 K) is 39.2 K lower than T_m (376.6 K), and the calculated ($T_m - T_A$) is larger than the typical relaxors PMN [22] or BST [24] (2–8 K). The frequency independent parameter δ can be used to characterize the width (dispersiveness) of the permittivity peak. The variations of δ and γ as functions of x are illustrated in Fig. 5. It is observed from Fig. 5 that with increasing BNMT contents there is a bimodal distribution of γ values. It is also observed that δ versus x has the same trend as γ versus x. The fitted parameters to the Lorenz relation for $(1 - x)$BT–xBNMT ceramics samples ($x = 0.2$–0.9) are listed in Table 2.

The degree of relaxation (in the frequency range 100 Hz–100 kHz) can be described by the parameter ΔT_{relax} as:

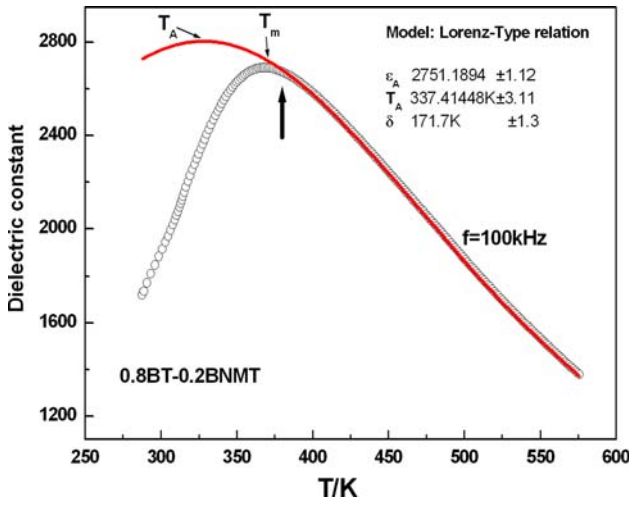

Fig. 4 Dielectric constants of 0.8BT–0.2BNMT as a function of temperature at 100 kHz. The *solid line* represents the fitting to the Lorenz-type relation. The *upward arrow* indicates the point of deviation upon decreasing of the temperature

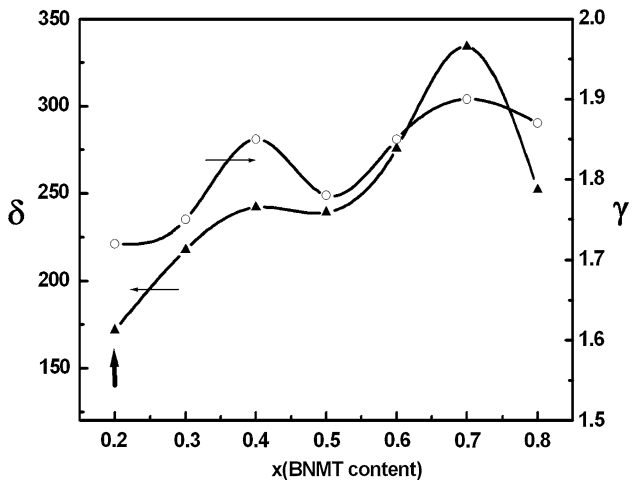

Fig. 5 The δ and γ of $(1 - x)$BT–xBNMT ($x = 0.2$–0.8) ceramics. The *upward arrow* at $x = 0.2$ indicates the onset of the relaxor behavior

Table 2 Summary of the fitted parameters of the Lorenz-type relation $\frac{\varepsilon_A}{\varepsilon} = \frac{(T-T_A)^2}{2\delta^2}$, for the dielectric peaks of $(1 - x)$BT–xBNMT ceramics

Composition x(BNMT)	ε_A	T_A (K)	δ (K)
0.8	2352	482	252[a]
0.7	2752	473	334[a]
0.6	2880	472	275.2
0.5	1723	450.7	239
0.4	2370	409.5	241
0.3	2362	366.4	217.9
0.2	2751	337	171.7

[a] The fittings are carried out in the temperature range from T_m to 110 K above the T_m

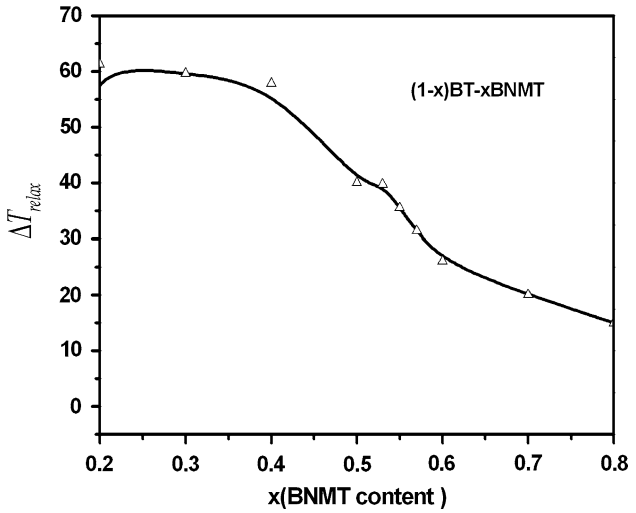

Fig. 6 The degree of relaxation $\left(\Delta T_{\text{relax}} = T_{\varepsilon_m(100\,\text{kHz})} - T_{\varepsilon_m(100\,\text{Hz})}\right)$ of $(1 - x)$BT–xBNMT ($x \sim 0.2$–0.8) ceramics

$$\Delta T_{\text{relax}} = T_{\varepsilon_m(100\,\text{kHz})} - T_{\varepsilon_m(100\,\text{Hz})}. \quad (3)$$

Figure 6 shows the calculated ΔT_{relax} for $(1 - x)$BT–xBNMT ($x = 0.2$–0.9) ceramics. The results show that ΔT_{relax} has a systematic decreasing trend with increasing x.

Temperature dependence of the relaxation time in $(1 - x)$BT–xBNMT ceramics system (x = 0.2–0.9)

It is believed that the so called polar nanoregions (PNRs) exist in the vicinity of T_m in any classical ferroelectric relaxor system. Each of those PNRs has a net polarization (P_s) with a characteristic relaxation time (τ) controlled by its local field configuration and its characteristic size. The energy barrier that prevents the switching of nano polarization states decreases as the size of the PNRs decreases. When the barrier height is low enough and becomes comparable to the thermal energy (kT), the directions of P_s fluctuate. In addition, the fluctuation of PNRs slows down (τ increases) with decreasing temperature [25]. It is proposed that the short-range interactions between the PNRs control the fluctuation of P_s, leading to its freezing at a characteristic temperature (freezing temperature). Similar to the spin glass systems the relaxation time (τ) in relaxors can be described by VF relation:

$$\tau = \tau_o \exp[-E/k_B(T - T_{VF})] \quad (4)$$

where τ is the relaxation time, τ_0 the pre-exponential factor, E the activation energy for relaxation, k_B the Boltzmann's constant, and T_{VF} the VF freezing temperature. As shown in Fig. 7, the temperature dependence of relaxation time fits well using VF relation for $(1 - x)$BT–xBNMT ceramics with $x = 0.2$, 0.3, and 0.4. However, for $x = 0.5$, 0.6, and 0.7, the fitted curves showed slight deviation from the experimental data. Although the curve fitted for $x = 0.5$, 0.6, and 0.7 are not ideal, the resulted E, T_{VF}, and τ_0 are still reasonable. As x increases to 0.8, the deviation diminishes but the fitted value T_{VF} is outside of the reasonable range. It is suggested from the aforementioned results that there are different types of relaxation phenomena occurring in these two composition regions.

In a previous study [11] of $(1 - x)$BT–xBNMT ceramics ($x = 0$–0.2) system on the crossover from normal ferroelectric to relaxor, it was shown that the relaxor behavior can be induced from the normal ferroelectric BT by an incorporation of BNMT; and that the ferroelectric relaxor behavior occurred at $x = 0.2$. The $(1 - x)$BT–xBNMT ceramics in the range of $x = 0.2$–0.9 can be considered as two interwoven ferroelectric relaxors, pure BNMT as a discrete phase and (0.8BT–0.2BNMT) as the matrix. This is an analogy of the case of BZT [26] system in which the polar ferroelectric BT distributes into the non-polar $BaZrO_3$ matrix, leading to the resulted dielectric characteristics. From previous studies of solid solution BZT, the temperature dependence of relaxation time fits well with VF relation for all of the BZT compositions that show relaxor behavior. The BZT system shows a gradual evolution of relaxor behavior with increasing content of polar BT in nonpolar $BaZrO_3$ [2, 27]. The mutual interaction among the polar regions, as well as the interaction between the polar and non-polar regions could be the source of random field, which induces the relaxor behavior [27].

Unlike BZT, both end members for $(1 - x)$BT–xBNMT are polar. In the range of $0.5 \leq x \leq 0.9$, the deviation from the VF relation can be hypothesized by the existence of more than one types of polar mechanism induced by the polar BNMT in the polar 0.8BT–0.2BNMT (relaxor) matrix. Alternatively, it can be stated that the deviation from the VF relation is due to multiple PNRs co-contribute to the resulted properties of the system after the concentration (percolation) threshold of each kind is reached. The resulted properties are the combination of relaxation behaviors contributed by each type of PNRs. However, in the range of $0.2 \leq x \leq 0.4$, the relaxation behavior is dominated by PNRs from 0.8BT–0.2BNMT, thus the curve fitting results in this region show good agreement with VF relation. Also when BNMT content increases, the activation energy decreases, and the freezing temperature and the relaxation time τ increase.

The fitting parameters of the VF relation of all compositions are summarized in Table 3.

Dielectric behavior of $(1 - x)$BT–xBNMT ceramics system: bias E-field dependence

The electric-field dependence of the permittivity of $x = 0.3$ at 100 kHz was measured from 19 to 105 °C and shown in

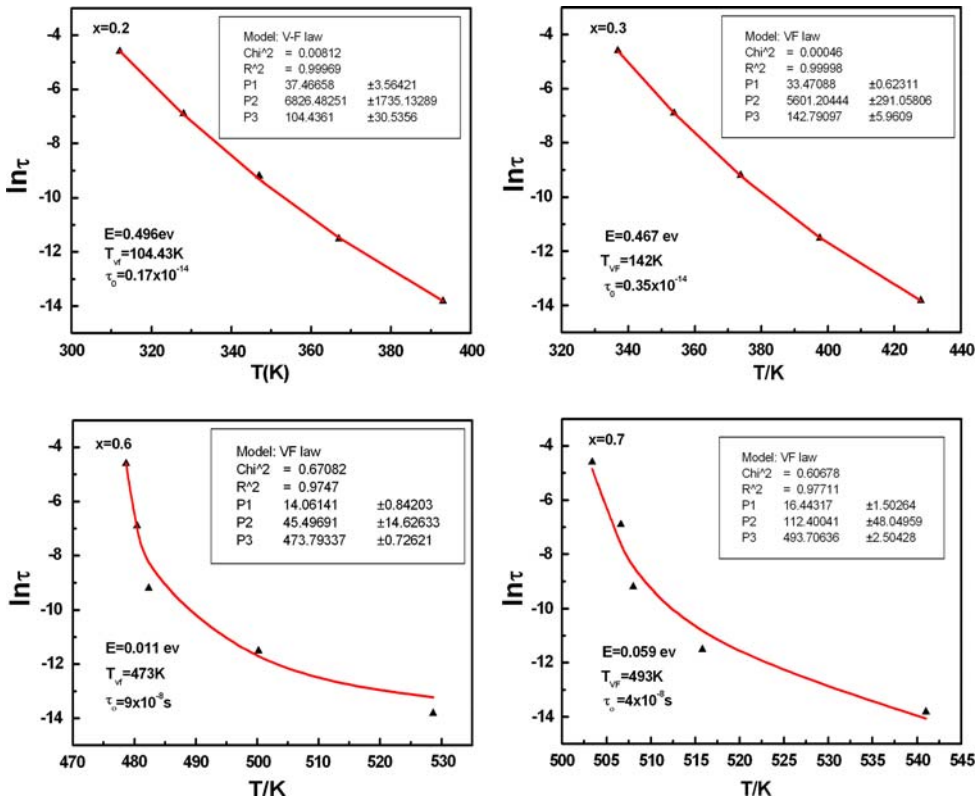

Fig. 7 Temperature dependence of relaxation time (τ) of $(1 - x)$BT–xBNMT ceramics, with $x = 0.2$–0.8. *Symbols* denote the experimental data and *solid curves* denote fitting to the VF relation

Table 3 Summary of the Vogel–Fulcher fitted parameters of $(1 - x)$BT–xBNMT ceramics

Composition	Freezing temperature (T_{VF}) (K)	Activation energy (E_a) (ev)	Preexponential factor (τ) (s)
0.2BT–0.8BNMT	542.12 ± 0.25	0.011	3.9×10^{-8}
0.3BT–0.7BNMT[a]	493.70 ± 2.0	0.059	4×10^{-8}
0.4BT–0.6BNMT[a]	473.79 ± 0.76	0.011	9×10^{-8}
0.5BT–0.5BNMT	334.22 ± 4.32	0.1239	1×10^{-11}
0.6BT–0.4BNMT	300.83 ± 18.77	0.124	1×10^{-11}
0.7BT–0.3BNMT	142.76 ± 5.96	0.467	0.35×10^{-14}
0.8BT–0.2BNMT	104.43 ± 30.56	0.496	0.17×10^{-14}

[a] Notable deviations from the experimental data were observed in the fitted results

Fig. 8. It is observed that ε' decreases non-linearly with the increasing electric field from 0 to 30 kV/cm.

The thermodynamic phenomenological treatments of the DC E-field dependence of ε' in polar dielectrics are established in the framework of LGD theory. According to LGD thermodynamic approach, for a polarizable but non-deformable crystal, the free energy can be written as [28, 29]:

$$G(P,T) = G(0,T) + \frac{\alpha}{2}P^2 + \frac{\beta}{4}P^4 + \frac{\gamma}{6}P^6 + \cdots, \quad (5)$$

where $\alpha = C(T - T_0) = 1/\varepsilon_0\varepsilon_r(0)$ is a temperature-dependent coefficient, T_0 the Curie–Weiss temperature, ε_0 the permittivity of free space, $\varepsilon_r(0)$ the relative dielectric constant at zero field, P polarization, and β and γ the coefficients independent of temperature. Notice that the coefficient γ in Eq. 5 is not the same as that in modified Curie–Weiss relation. The Eq. 5 after introducing Johnson's assumption [29] of a small polarization $P = \varepsilon_r(E)\varepsilon_0 E$ (in this case, the P^4 and above terms are neglected) can be rewritten as:

$$\varepsilon_r(E) = \varepsilon_r(0)/\{1 + \lambda[\varepsilon_0\varepsilon_r(0)^3E^2]\}^{1/3} \quad (6)$$

where $\lambda = 3\beta$.

On further simplification, the dielectric behavior in a paraelectric state in the ferroelectric under low DC electric-field can be expressed as [29, 30]:

$$\begin{aligned}\varepsilon_r(E) &= \varepsilon_r(0)/\{1 + \lambda[\varepsilon_0\varepsilon_r(0)^3E^2]\}^{1/3} \\ &= \varepsilon_1 - \varepsilon_2E^2 + \varepsilon_3E^4 - \varepsilon_4E^6 + \varepsilon_5E^8 - \cdots\end{aligned} \quad (7)$$

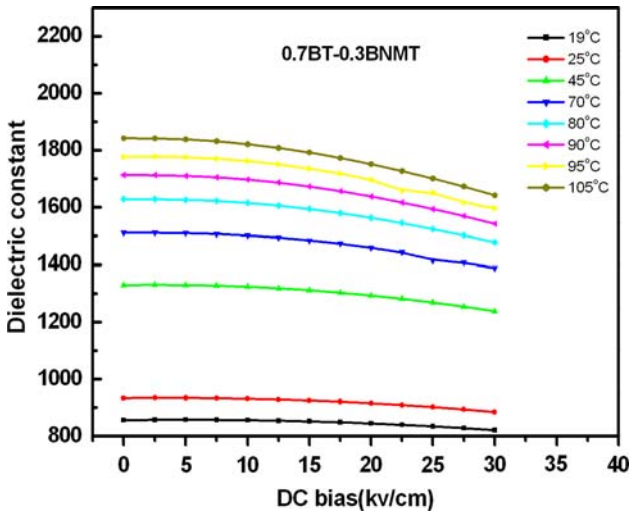

Fig. 8 Dielectric constants of 0.7BT–0.3BNMT as function of bias electric-fields at different temperatures

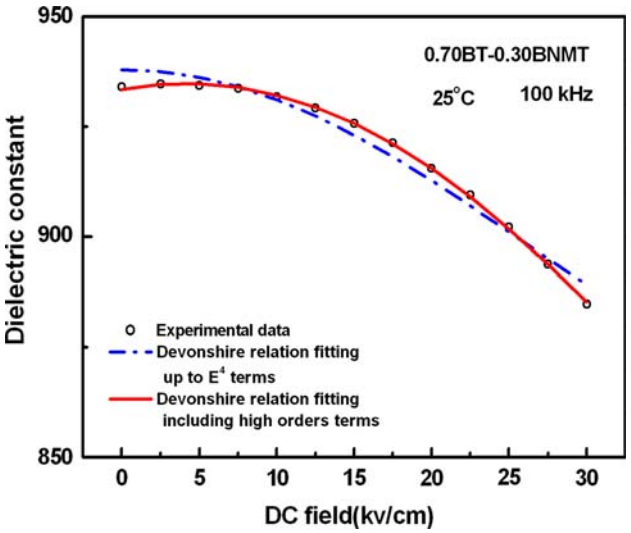

Fig. 9 *E*-field dependence of dielectric constant of 0.7BT–0.3BNMT at 100 kHz. The experimental data are denoted in *open circles*. The *dashed line* is the fitted curve according to Eq. 7 (not including E^4 and higher terms). The *solid line* is the fitted curve including the terms higher than E^4 in Eq. 7

where $\varepsilon_1 = \varepsilon_r(0)$, $\varepsilon_2 = \frac{1}{3}\lambda\varepsilon_r(0)\varepsilon(0)^3$, $\varepsilon_3 = \frac{2}{9}\lambda^2\varepsilon_r(0)\varepsilon(0)^6$, $\varepsilon_4 = \frac{14}{81}\lambda^3\varepsilon_r(0)\varepsilon(0)^9$, $\varepsilon_5 = \frac{35}{243}\lambda^4\varepsilon_r(0)\varepsilon(0)^{12}$, etc. where ε_1 is the linear dielectric constant. ε_2, ε_3, and higher order terms are the non-linear dielectric constants, respectively, which are all temperature dependent. A similar treatment has also been adopted to analyze DC dependence of the specific heat by Lawless [31]. Equation 7 has been widely adopted to analyze the dielectric-field dependence behavior of non-linear dielectrics other than proper ferroelectric [32, 33].

For $x = 0.3$ composition, poor fit of the resulted $\varepsilon(E)$ was observed if the high order terms (E^4 and higher) are omitted. However, results calculated including higher order terms produce good fits in describing the electric-field dependence of the permittivity as shown in Fig. 9. The fitting parameters obtained are $\varepsilon_1 = 2101.4$, $\varepsilon_2 = 0.01356\ (\mathrm{V/m})^{-2}$, $\varepsilon_3 = 0.2 \times 10^{-4}\ (\mathrm{V/m})^{-4}$, $\varepsilon_4 = 4.8 \times 10^{-6}\ (\mathrm{V/m})^{-6}$, $\varepsilon_5 = 2.3 \times 10^{-8}\ (\mathrm{V/m})^{-8}$, and $\lambda = 3\beta = 3.1 \times 10^{23}\ (\mathrm{Vm^5/C^3})$.

In many polar relaxors, *E*-field dependence of $\varepsilon(E)$ should include the contribution from the reorientation of polar-clusters. The Langevin-type polar cluster contribution is thus to be taken into account for higher order dielectric response [34]. By means of the Langevin approach, the total polarization of a cluster system can be expressed as [35]:

$$P_c = P_r \tanh(P_r L^3 E/2k_B T) \tag{8}$$

where P_r is the effective polarization of polar clusters, L the cluster size, and E the electric field considered. In the present work, the following simplified combination equation is adopted to analyze the field dependence of the dielectric constant for $(1-x)$BT $-$ xBNMT ceramics:

$$\varepsilon(E) = \varepsilon_1 - \varepsilon_2 + \varepsilon_3 E^4 + [P_r x/\varepsilon(0)][\cosh(Ex)]^{-2} \tag{9}$$

where $x = P_r L^3 E/2k_B T$. The Langevin-type term of the right hand side of Eq. 8 describes the cluster contribution. The fitting curve obtained is in good agreement with the experimental data for the composition $x = 0.3$ as shown in Fig. 10. The polarization of the polar clusters was calculated to be $P \sim 6.2$–$9.8\ \mu\mathrm{C/cm^2}$ with the clusters size $L \sim 4$–8 nm by Eq. 9. The existence of such polar clusters may also underline that the compositions of $(1-x)$BT–xBNMT system, which shows dielectric relaxation behavior are in fact ferroelectric relaxors.

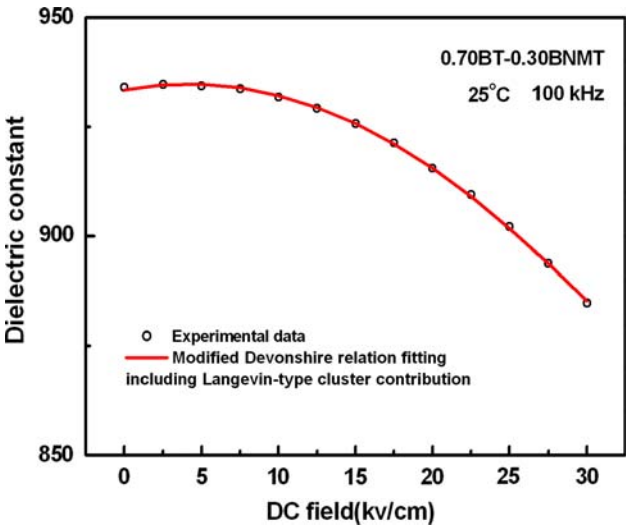

Fig. 10 *E*-field dependence of the dielectric constant of 0.7BT–0.3BNMT at 100 kHz. *Open circles* are the experiment data. The *solid curve* is the fitted result by the combination of LGD and Langevin relation

Conclusion

In summary, this article reports the dielectric properties and relaxor ferroelectric behavior of the solid solution between BT and BNMT. Samples with compositions across the solid solution range between end members, $(1 - x)$BT–xBNMT ($x \sim 0.2$–0.9), are prepared by a solid-state reaction method and the dielectric permittivities and losses are measured as functions of temperature, frequency, and bias E-field. All compositions are confirmed to form perovskite structure by X-ray powder diffraction measurements and can be indexed in pseudo-cubic lattices. Diffuseness parameters, γ and δ, are calculated from fits of the dielectric data using a modified Curie–Weiss law and an empirical Lorenz-type relation under zero-field conditions. The results indicate an interesting evolution of relaxor behavior showing two composition regions where the diffuseness parameters exhibit maxima. The VF relation fits well for $(1 - x)$BT–xBNMT ceramics with $x = 0.2$, 0.3, and 0.4. However, for $x = 0.5$, 0.6, 0.7, and 0.8, the fitting curves show slight deviation from the experimental data. The results also support the hypothesis that there are different types of relaxation phenomena occurring in these two composition regions. The curve fits of the bias E-field dependence of the permittivity using LGD polynomial expansion (with higher order terms) appear to confirm the relaxor ferroelectric behavior of the system. In addition, calculations of LGD by substituting higher order terms with Langevin-type relation also support this hypothesis. The nano polar clusters are calculated to be $P \sim 6.2$–9.8 $\mu C/cm^2$ for sizes on the order of a few nanometers ($L \sim 4$–8 nm). Although $(1 - x)$BT–xBNMT ($x = 0.2$–0.9) ceramics have moderate dielectric constant values (maximum $\sim$2000), study of this system expands the understanding to a new relaxor ferroelectric system (0.8BT–0.2BNMT) consisting of ferroelectric (BT) and relaxor ferroelectric (BNMT) end members. Further investigations on the electrical response, such as pyroelectricity, piezoelectricity, and electrostriction, are in progress to understand the nature of the clusters responsible for polarization and electromechanical behavior.

Acknowledgement This work has been supported by US National Science Foundation under grant number NSF 0833000 and by US Office of Naval Research under grant number N00014-08-1-0854. One of the authors acknowledges the support of National Natural Science Foundation of China (Project 50772087) and scholarship from China Scholar Council through the program of National study-abroad project for postgraduates of high level universities.

References

1. Bokov AA, Ye Z-G (2006) J Mater Sci 41:31. doi:10.1007/s10853-005-5915-7
2. Bokov AA, Ye ZG (2002) Phys Rev B 66:064103
3. Cross LE (1987) Ferroelectrics 76:241
4. Maiti T, Guo R, Bhalla AS (2006) J Appl Phys 100:114109
5. Maiti T, Guo R, Bhalla AS (2007) Appl Phys Lett 90:182901
6. Maiti T, Guo R, Bhalla AS (2006) Appl Phys Lett 89:122909
7. Tiwari VS, Singh N, Pandey D (1995) J Phys Condens Matter 7:1441
8. Singh N, Pandey D (1996) J Phys Condens Matter 8:4269
9. Singh N, Singh AP, Parsad CD, Pandey D (1996) J Phys Condens Matter 8:7813
10. Wang X, Cao W (2007) J Eur Ceram Soc 27:2481
11. Wu L, Wang X, Wang JH, Guo R, Bhalla AS (2009) Ferroelectr Lett 36:28
12. Vogel H (1921) Phys Z 22:645
13. Fulcher GS (1925) J Am Ceram Soc 8:339
14. Tholence JL (1980) Solid State Commun 35:113
15. Johnson KM (1961) J Appl Phys 33:2826
16. Drougard ME, Landauer R, Young DR (1955) Phys Rev 98:1010
17. Stern E, Lurio A (1961) Phys Rev 123:117
18. Rupprecht G, Bell RO (1964) Phys Rev 135:A748
19. Langevin P (1905) J Phys 4:678
20. Uchino K, Nomura S (1982) Ferroelectrics 44:55
21. Bokov AA, Ye ZG (2000) Solid State Commun 116:105
22. Bokov AA, Bing YH, Chen W, Ye ZG, Bogatina SA, Raeviski IP, Raevskaya SI, Sahkar EV (2003) Phys Rev B 68:052102
23. Viehland D, Jang S, Cross LE, Wittig M (1991) Phil Mag B 64:335
24. Lei C, Bohov AA, Ye Z-G (2007) J Appl Phys 101:084105
25. Samara GA (2003) J Phys Condens Matter 15:367
26. Matit T, Guo R, Bhalla AS (2008) J Am Ceram Soc 91(6):1769
27. Dixit A, Majumder AB, Katiyar RS, Bhalla AS (2006) J Mater Sci 41:87. doi:10.1007/s10853-005-5929-1
28. Burfoot JC, Taylor GW (1979) Polar dielectrics and their applications. Macmillan Press Ltd, London
29. Lines ME, Glass AM (1977) Principle and application of ferroelectrics and related materials. Oxford University Press, Oxford
30. Devonshire AF (1949) Phil Mag 40:1040
31. Lawless WN (1977) Phys Rev B 16:433
32. Bianchi U, Dec J, Kleemann W, Bednorz JG (1995) Phys Rev B 51:8737
33. Chaves MR, Almeida A, Maglione M, Ribeiro JL (1996) Phys Status Solid B 197:503
34. Ang C, Cross LE, Guo R, Bhalla AS (2000) Appl Phys Lett 77:732
35. Bell AJ (1993) J Phys Condens Matter 5:8773